ELSEVIER

Diamond and Related Materials 10 (2001) 1125–1131

DIAMOND AND RELATED MATERIALS

www.elsevier.com/locate/diamond

Dual ion plasma-beam sources used to maximise sp^3 C–C bonds in carbon nitride

S.E. Rodil[a,*], W.I. Milne[a], J. Robertson[a], L.M. Brown[b]

[a] *Engineering Department, Cambridge University, Trumpington Street, Cambridge CB2 1PZ, UK*
[b] *Cavendish Laboratory, Cambridge University, Cambridge CB3 0HE, UK*

Abstract

Amorphous carbon nitride films grown by plasma or ion sources never achieve the limit of β-C_3N_4, because the nitrogen fraction saturates below 57% and the carbon tends to become sp^2-bonded at high N content. When a-CN_x is grown from a single ion or plasma beam, high nitrogen pressures are needed to promote higher N contents, but this leads to a loss of ionisation. We use a dual ion beam method to grow a-CN_x with a filtered cathodic arc (FCVA) to supply carbon and a low pressure, high plasma density electron cyclotron wave resonance (ECWR) source to supply atomic nitrogen ions. The film composition and fraction of unsaturated π^* bonding at C and N sites was measured by electron energy loss spectroscopy. We find that the C sp^3 fraction decreases linearly with nitrogen content, rather than showing the sharp fall at $N/C = 0.08–0.1$ found by others. Thus, we achieve the highest C–C sp^3 content for a-CN_x films with $N/C > 0.1$. We find a rather sharp increase in the fraction of empty N π^* states, from 10 to 30% at $N/C = 0.2$. Whereas previous work suggests that N contents above the critical value of 0.1 induce a transition for all C sites to sp^2, in our results only those C sites bonded to N revert to sp^2. The film density was observed to change in a similar way to the density of ta-C films with respect to the C sp^2 fraction. However, strong differences in the optical gap are observed.

Keywords: Diamond-like carbon (DLC); Carbon nitride; sp_3 bonding; Deposition

1. Introduction

The prediction that β-C_3N_4 will have a hardness comparable to diamond [1] has been the driving force in the research on carbon nitride. Both chemical and physical vapour deposition-based (CVD and PVD) techniques have been tried [2–7]. However, most synthesis methods create amorphous a-CN_x films with x values below the desired 4/3 and with little sp^3 carbon bonding at moderate N contents.

Different carbon nitride crystalline phases have been studied theoretically [8], among those β- and α-C_3N_4 are dense, and metastable phases in which the bonding is sp^3 at the carbon site and sp^2 plus p^2 at the nitrogen site. It is now well established that to grow dense metastable phases it is necessary to use highly ionised plasma beams with ions of medium energy in which the ions penetrate the surface layer (subplantation), leading to the subsurface growth of a densified, quenched-in phase [9,10]. Subplantation has been used to grow the highly sp^3-bonded tetrahedral amorphous carbon (ta-C) [11] and cubic boron nitride [12]. This same process has been applied to a-CN_x by alternating mass-selected ion beams (MSIB) of C^+ and N^+ ions [13] or two Kaufman sources [14]. Alternatively, pulsed laser deposition

* Corresponding author. Tel.: +44-1223-332679; fax: +44-1223-332662.
E-mail address: ser26@eng.cam.ac.uk (S.E. Rodil).

0925-9635/01/$ - see front matter
PII: S0925-9635(00)00527-6

(PLD) [15] or filtered cathodic vacuum arc (FCVA) [16–18] has been used to ablate a graphite target, producing a highly ionised carbon beam under nitrogen background pressure. However, in order to increase the nitrogen content in the films, a high N_2 pressure must be used, leading to a lower ionisation and a loss of subplantation efficiency, with a subsequent reversion to C sp^2 bonding. Generally, the explanation given for the increase in the C sp^2 bonding, even at N contents less than 1 at.%, was that nitrogen destabilises all the carbon sp^3 network [16,19].

In this work, we study the effect of the nitrogen partial pressure on the ionisation of the carbon beam of a FCVA system, showing that pressure acts as a plasma limit on the subplantation growth process. In order to identify the real effect of nitrogen bonding into the amorphous carbon network, we deposited CN films using a highly efficient, low-pressure N_2 plasma beam, together with the FCVA system, in a similar way to ion-assisted deposition techniques [19–22].

2. Experimental

A single-bend FCVA system was used as the carbon ion source. The average ion self-energy of the C ions was 25–30 eV, sufficiently high to produce ta-C films with 85% sp^3 bonding, so no substrate bias was used. In order to determine the effect of chamber pressure on the C ion flux a Faraday cup mounted on the substrate plane was used. The chamber pressure was varied by increasing the flow-rate of nitrogen gas in the chamber and monitored by a Penning gauge.

The nitrogen ion beam was produced by a high-density plasma source called an electron cyclotron wave resonance source (ECWR) [23]. The ECWR source operates at low pressure and provides a nitrogen ion beam with a high degree of dissociation, in which the N^+/N_2^+ ratio varies depending on operation parameters [23]. The energy of the ions was varied between 60 and 100 eV, sufficient to cause subplantation, but not too high to give chemical sputtering, which has been proven to be a cause of reduced N incorporation [24,25].

a-CN_x films with different N content were deposited by changing the relative position of the substrate holder with respect to the sources, and therefore the C/N ion flux impinging on the substrate. Initially, the substrate was placed facing the FCVA; thus, the nitrogen ions impinge at 45°. By increasing the distance between the holder and the FCVA, the C current density decreased to half its initial value and the nitrogen current density was three-fold higher. This led to films with a nitrogen content up to 35 at.%. Then, the films with N content above 35% were deposited by slightly rotating the sample holder in order to further increase the nitrogen current density. At this point, both ions impinged with an angle $< 45°$ with the substrate. This small angle has no strong effect on the sp^3 C–C bonding, and this was previously determined by depositing ta-C films at different angles. The C current density at 45° reduced to one third of its value at normal incidence and the reduction in the C sp^3 was only 10%. However, in the case of CN deposition, it is important to note that any decrease in the C current density is compensated by an increase in the N current density, therefore the films are always under ion bombardment. The chamber pressure was maintained below 5×10^{-4} mbar to avoid loss of ionisation of the C ion flux, as determined previously.

The N/C composition ratio (x), the C sp^3 content, the fraction of empty π^* states ($f_N(\pi)$) and the mass density were determined by electron energy loss spectroscopy (EELS). The CN films were chemically removed from the Si substrate, rinsed and floated onto Cu microscope grids. EELS measurements were made in a Vacuum Generators HB501 scanning transmission electron microscope with a dedicated parallel EELS spectrometer of the McMullan design. All spectra were collected at a convergence angle of 7.4 mrad, and an acceptance angle of 7 mrad, for 100 keV. This ensures that all sample directions were equally probed at the K edge energy, so the results are independent of any anisotropy in the film [26]. Both low-loss (< 50 eV) and high-loss spectra were collected, with high-loss spectra taken for both C K and N K ionisation edges. The resultant spectrum is an average for a series of up to 40 spectra acquired from the same position. No degradation of the films was observed during the measurements, indicating a good degree of film stability to electron irradiation.

The optical gap was obtained for films deposited on Corning glass by transmission and reflection measurements using an ATI-Unicam UV2-200 spectrometer in the range 300–1100 nm.

3. Results

The carbon ion current density as a function of the nitrogen partial pressure is shown in Fig. 1, in which it is evident that an order of magnitude increase in nitrogen pressure leads to an even larger decrease in ion current, from 0.4 to 0.01 mA/cm^2. Films deposited under these conditions show a decrease in C sp^3 fraction from 85 to 60%, and a very low N incorporation. Therefore, the main experiments using both sources maintained the nitrogen pressure below 5×10^{-4} mbar.

EELS spectra of films with different N content are shown in Fig. 2. The spectra have been corrected by removing the background intensity and by deconvolu-

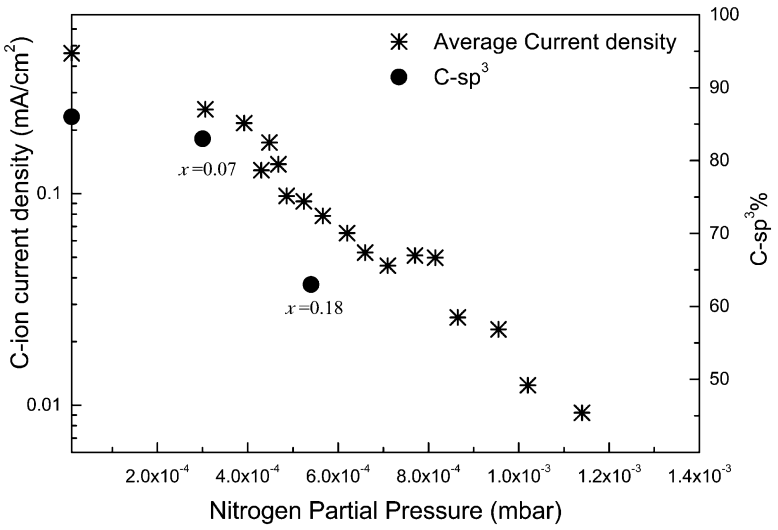

Fig. 1. Ion current density and carbon sp^3 fraction as a function of the nitrogen pressure. The current density is the average obtained for up to 50 runs to allow for fluctuations in the plasma. The stoichiometry of the a-CN_x samples is also indicated.

tion of up to five multiple scattering processes. The N/C composition ratio was derived from the relative areas of the N and C K edges, using the partial cross-sections calculated using the Egerton hydrogenic model [27]. The stoichiometry is quoted as CN_x where $x = N/C$ is the composition ratio determined directly from EELS. However, assuming that there are not any other elements in the samples, as was confirmed by nuclear reaction analysis of a few samples, the N% can be estimated as $N\% = x/(1+x)$. The energy loss spectra for all films look similar, with broad features reflecting the amorphous nature of the films. Transitions from the core level electrons to σ^* states occur at 290 eV for C and 410 eV for N, forming the ionisation edges. The pre-peak, or shoulder, preceding the edges is due to transitions to π^* antibonding states from sp^2 and sp^1 sites [27,28].

Fig. 3 shows the C sp^3 fraction as a function of x, derived from the C K edge spectra, and deserves special attention. The π^* peak corresponds to the sum of sp^2 sites plus twice the sp^1 sites (which have two π states). For carbon films, sp^1 sites are very uncommon and can be neglected in sp^3 estimations; however, this is not the case in a-CN_x [29,30]. As a first approximation, we neglect sp^1 states, since the intensity of C≡N modes in both our Raman and IR spectra is very low [31]. The C sp^3 fraction is derived as $1 - f_C(sp^2)$, where

$$f_C(sp^2) = \frac{(I_{\pi*}/I_w)_{sample}}{(I_\pi/I_w)_{graphite}} \quad (1)$$

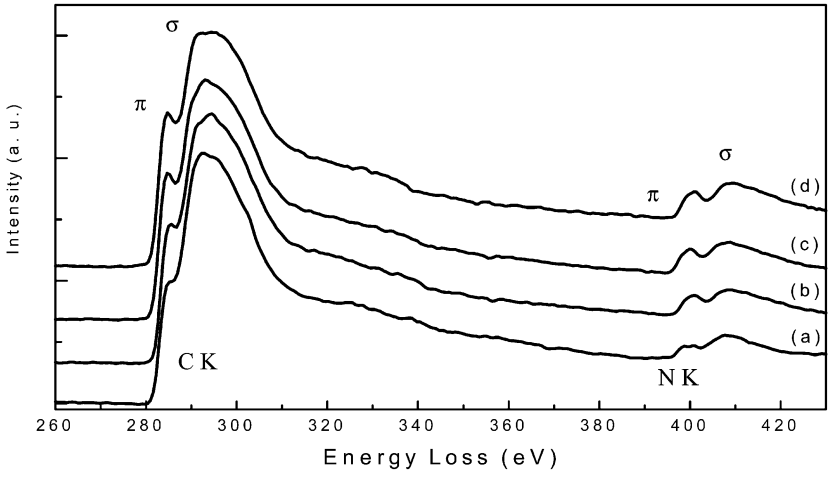

Fig. 2. High-loss electron energy loss spectra for samples deposited at different distance from the FCVA. The spectra are normalised in a window away from the edge, so the intensity reflects the change in π bonds and nitrogen content. (a) 7 cm, $x = 0.26$; (b) 9.5 cm, $x = 0.3$; (c) 11 cm, $x = 0.37$; and (d) 14.5 cm, $x = 0.41$.

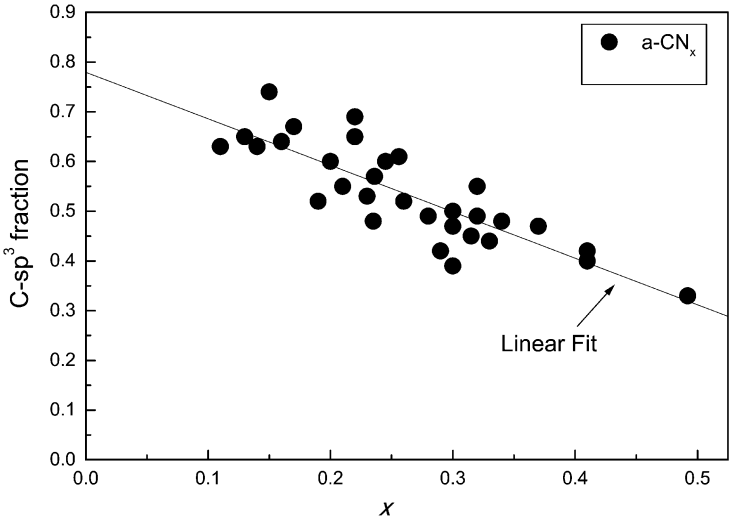

Fig. 3. Carbon sp^3 fraction as a function of the composition ratio, x.

I_{π^*} is the integrated area under the π^* peak and I_w is the integrated area over a defined energy window (283.4–294) in the spectrum [32]. The values obtained for $f_C(sp^2)$ are less than unity for all the samples, demonstrating that the fraction of sp^1 states is negligible [21,33].

It is also important to note that the fraction of sp^3 sites measured by EELS is independent of whether carbon is bonded to C or N. Therefore, sp^2 C=N groups decrease the overall sp^3-bonded C fraction. The C sp^3 fraction decreases linearly from 85% for N-free samples to $\sim$40% for the most nitrogenated sample, a-$CN_{0.5}$.

Nitrogen bonding is analysed qualitatively. The normalised area of the N π^* peak is indicative of the number of nitrogen empty π^* states, $f_N(\pi)$ calculated as:

$$f_N(\pi) = \frac{I_{\pi^*}}{I(_{\text{window}})} \quad (2)$$

where I_{π^*} is the area over the whole π^* peak and $I_{(\text{window})}$ is the integrated area over a defined energy window (395–409) in the spectrum.

An increase in $f_N(\pi)$ suggests a larger fraction of unsaturated sp^2 (neglecting sp^1) bonds; however, it is not possible to obtain an absolute value, unless a standard material is used for comparison. Fig. 4 shows $f_N(\pi)$ as a function of the composition ratio. Regardless of the dispersion in the data, two regions can be clearly distinguished, indicating a change in the N bonding configuration.

The film density is estimated from the low-energy loss spectrum. The plasmon peak is due to resonant oscillations of the $(\sigma+\pi)$ electrons, and the energy position or plasmon energy is proportional to the valence electron density of the material [27]. The mass density is then derived from the valence electron density, assuming that carbon contributes four valence electrons and nitrogen five, and assigning an effective electron mass of 0.85 [34]. We use five valence electrons for N because the density obtained agrees very well with the density measured by X-ray reflectivity in some samples [35]. This contrasts with Si_3N_4 samples, where the density is derived from the plasmon energy using three valence electrons per nitrogen atom [36]. The variation in the mass density as a function of the measured C sp^3 fraction is plotted in Fig. 5. The density decreases from $\sim$3.0 to 2.4 g/cm^3 as the nitrogen content and the C sp^2 fraction increase to 0.5 and 40%, respectively.

The Tauc optical gap was estimated by plotting the variation of $\sqrt{\pi E}$ against the energy, E, where α is the absorption coefficient, and then performing a linear extrapolation to the x-axis. Fig. 6a,b shows the optical gap as a function of the N/C composition ratio and the C sp^2 fraction, respectively. Because of the linear relationship between N/C and C sp^2 fraction, both plots present the same trend. The optical gap falls sharply from 2.4 eV for the ta-C sample to approximately 1 eV and then remains almost constant for further nitrogen incorporation, independent of the increase in the C sp^2 fraction.

4. Discussion

We find that the C sp^3 fraction decreases linearly with the N content rather than showing the sharp fall at low N content found by other groups and attributed to a nitrogen-induced C sp^3 to sp^2 transition [19]. The sp^3 to sp^2 transition is due, not only to the N content, but also to the low ionisation of the beams. In particular, when a FCVA system is used to ionise the N_2 gas,

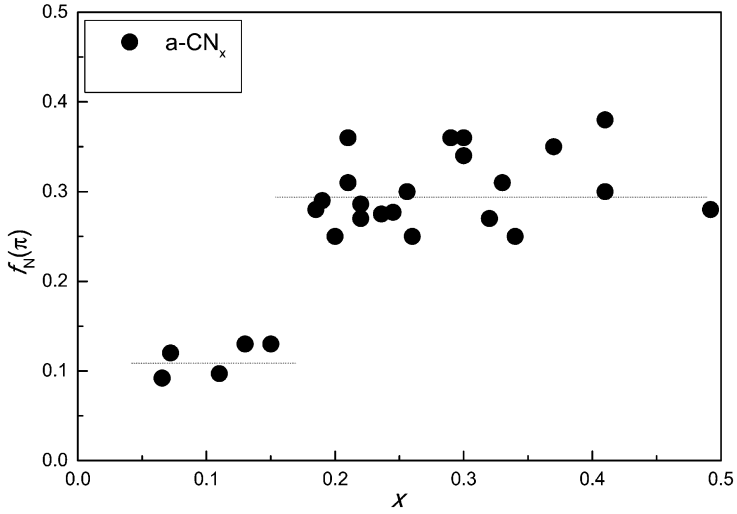

Fig. 4. Relative fraction of N empty π^* states vs. composition. The vertical scale is only for comparison purposes, and does not mean than only 30% N atoms have unsaturated bonds.

the transition is mainly due to the neutralisation of the carbon beam. When the pressure in the chamber is increased, the mean free path of the ions is reduced, then most of the ions recombine, forming neutral species before reaching the substrate plane. Thus, the film growth is controlled by neutral species and no subplantation occurs.

A linear fit of the C sp^3 fraction as a function of x gives:

$$C\ sp^3 = 0.78 - 0.94x \quad (3)$$

Eq. (3) gives a C sp^3 fraction for a N-free sample of $\sim 80\%$, consistent with ta-C films. The slope in Eq. (3) represents the rate of decrease of the sp^3 fraction. This rate is very close to unity, suggesting that all the carbon atoms which are bonded to nitrogen revert to sp^2, i.e. C=N double bond are formed, instead of C–N single bonds. A sp^3-CC to sp^2-CN transformation was also suggested for ion-assisted PLD-CN samples [20].

On the other hand, Fig. 4 shows a sharp transition for the N bonding. At $x < 0.2$, there are less N π^* states; however, we cannot conclude how N is bonded, since there are two possible N bonding configurations with no π electrons. In the first, N atoms are sp^2 in the bonding plane with a filled p^2 π lone-pair orbital normal to the bonding plane, as in β-C_3N_4 (or β-Si_3N_4). Thus, there are no empty N π^* states. In the other, N substitutes C atoms in a four-fold configuration, giving one electron for doping (N_4^+ sites) and no empty π^*

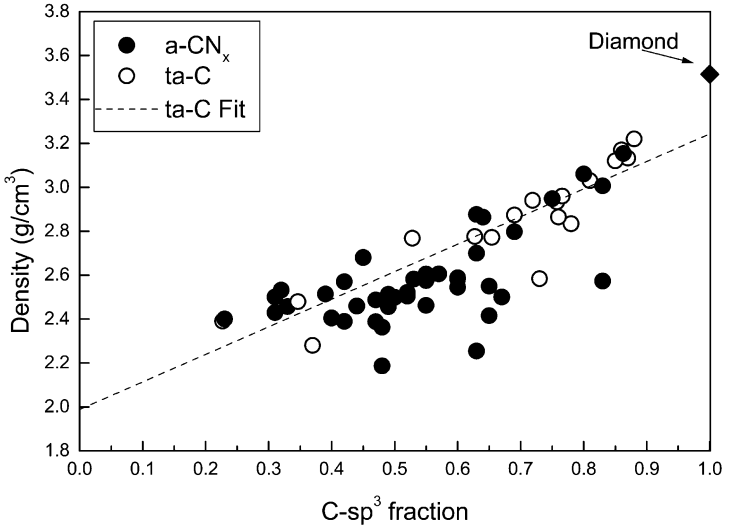

Fig. 5. Mass density for all the a-CN_x films as a function of the measured C sp^3%.

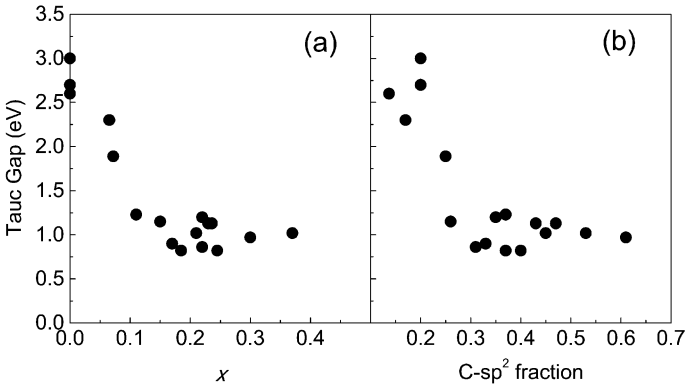

Fig. 6. Optical gap as a function of: (a) N/C composition ratio; and (b) C sp^2 fraction.

states [37]. As x exceeds 0.2, more unsaturated π^* states appears, $f_N(\pi)$ increases and remains approximately constant for higher x. In general, however, there are many unsaturated N configurations in a-CN_x, ranging from aromatic (pyridine or pyrrole) to C=N groups and nitrile (C≡N) groups that can contribute to the $f_N(\pi)$ fraction.

The overall dependence of the C and N bonding on x suggests that, at low nitrogen concentrations, N atoms tend to substitute for C atoms in either sp^3 or sp^2 sites. However, at higher x, the formation of C=N bonds is chemically favourable [38], leading to a reduction in the measured C sp^3 fraction.

In contrast with the results obtained by Wan and Egerton [33], the density of the a-CN_x films is seen to vary linearly with the C sp^3 fraction, in a similar way to that found for ta-C [34]. This similar trend suggests that the gross effect of N incorporation in the network connectivity is to decrease the carbon co-ordination number as the number of C=N double bonds increases.

On the other hand, the electronic configuration of the carbon nitride samples is definitely different to that of amorphous carbon, and this is reflected in the optical gap variation. For amorphous carbon films, either hydrogenated or not, the optical gap depends on both the distribution and quantity of the sp^2 phase, since the gap is controlled by the π electron delocalisation, not only in ordered rings, but in the whole sp^2 phase. However, for the ta-CN_x samples presented here, the gap remains constant at approximately 1 eV, even though the C sp^2 fraction increases from 30 to 50%. Therefore, there must a different mechanism which induces localisation of the π electrons.

5. Conclusions

We have used a two-beam plasma system at low operating pressure to produce carbon nitride films with ~45 at.% N, a moderate fraction of C sp^3 bonding (40%) and densities above 2.0 g/cm^3. However, it is still far away from the predicted β-C_3N_4, since we would achieve 100% sp^2 bonding at a nitrogen content less than 57%. Moreover, we can conclude that the previously suggested nitrogen-induced sp^3 C–C to sp^2 C=C transition, where above a certain N concentration all C atoms revert to sp^2 bonding, is more a consequence of the growth process than of the N content. In our work, using separate ion sources for C and N species, where subplantation is still efficient, only those carbon atoms directly bonded to N revert to sp^2 bonding, which gives a sp^3 C–C to sp^2 C=N transition linear in N content.

Acknowledgements

S.E. Rodil acknowledges CONACYT and the ORS award scheme for a postgraduate scholarship.

References

[1] A.Y. Liu, M. Cohen, Science 24 (1989) 841.
[2] D. Franceschini, F.L. Freire, G. Mariotto, Proceedings of the 1st International Specialist Meeting on Amorphous Carbon, 'Amorphous Carbon, State of the Art', World Scientific, Singapore, 1998, p. 130.
[3] S.F. Yoon, Rusli, J. Ahn, Q. Zhang, H. Yang, F. Watt, Thin Solid Films 340 (1999) 545.
[4] K.J. Boyd, D. Marton, S.S. Todorov et al., J. Vac. Sci. Technol. A 13 (1995) 2110.
[5] D. Marton, K.J. Boyd, J.W. Rabalais, Int. J. Mod. Phys. B9 (1995) 3527.
[6] S. Muhl, J.M. Mendez, Diamond Relat. Mater. 8 (1809) 1999.
[7] N. Hellgren, K. Macak, E. Broitman, M.P. Johansson, L. Hultman, J.E. Sundgren, J. Appl. Phys. 88 (2000) 524.
[8] D.M. Teeter, R.J. Hemley, Science 271 (1996) 53.
[9] Y. Lifshitz, S.R. Kasi, J. Rabalais, Phys. Rev. Lett. 68 (1989) 620.
[10] J. Robertson, Diamond Relat. Mater. 3 (1994) 361.
[11] P.J. Fallon, V.S. Veerasamy, C.S. Davis et al., Phys. Rev. B 48 (1993) 4777.
[12] J. Robertson, Diamond Relat. Mater. 5 (1996) 519.
[13] D. Marton, K.J. Boyd, A.H. Al-Bayati, J.W. Rabalais, Phys. Rev. Lett. 73 (1994) 118.

[14] P. Hammer, M.A. Baker, C. Lenardi, W. Gissler, J. Vac. Sci. Technol. A 15 (1) (1997) 107.
[15] E. D'Anna, M.L. De Giorgi, A. Luches, M. Martino, A. Perrone, A. Zocco, Thin Solid Films 347 (1999) 72.
[16] C.A. Davis, D.R. Mackenzie, Y. Yin, E. Kravtchinskaia, G.A.J. Amaratunga, V.S. Veerasamy, Phil. Mag. B 69 (1994) 1133.
[17] X. Shi, H. Fu, J.R. Shi, L.K. Sheah, B.K. Tay, P. Hui, J. Phys.: Condens. Matter 10 (1998) 9293.
[18] B. Kleinsorge, A.C. Ferrari, J. Robertson, W.I. Milne, J. Appl. Phys. 88 (2000) 1149.
[19] J. Hu, P. Yang, C. Lieber, Phys. Rev. B 57 (1998) 3185.
[20] C. Spaeth, M. Kuhn, F. Richter et al., Diamond Relat. Mater. 7 (1998) 1727.
[21] K. Yamamoto, Y. Koga, S. Fujiwara, F. Kokai, J.I. Kleiman, K.K. Kim, Thin Solid Films 339 (1999) 38.
[22] S. Bhattachatyya, O. Madel, S. Schulze, P. Häussler, M. Hietschold, F. Richter, Phys. Rev. B 61 (2000) 3927.
[23] M. Weiler, K. Lang, E. Li, J. Robertson, App. Phys. Lett. 72 (1998) 1314.
[24] P. Hammer, W. Gissler, Diamond Relat. Mater. 5 (1996) 1152.
[25] S.E. Rodil, N.A. Morrison, J. Robertson, W.I. Milne, Phys. Status Solidi A 174 (1999) 25.
[26] N.K. Menon, J. Yuan, Ultramicroscopy 74 (1998) 83.
[27] F. Egerton, Electron Energy Loss Spectroscopy in the Electron Microscope, 2nd, Plenum Press, New York, 1996.
[28] K.W.R. Gilkes, J. Yuan, G.A.J. Amaratunga, Diamond Relat. Mater. 5 (1996) 560.
[29] J.H. Kaufman, S. Metin, D.D. Saperstein, Phys. Rev. B 39 (1989) 13053.
[30] N.M. Victoria, P. Hammer, M.C. dos Santos, F. Alvarez, Phys. Rev. B 61 (2000) 1083.
[31] S.E. Rodil, A.C. Ferrari, W.I. Milne, J. Robertson, in preparation.
[32] P.J. Fallon, Ph.D. Thesis, Cambridge University, 1992.
[33] L. Wan, R.F. Egerton, Thin Solid Films 279 (1996) 34.
[34] A. LiBassi, A.C. Ferrari, V. Stolojan, B.K. Tanner, J. Robertson, L.M. Brown, Diamond Relat. Mater. 9 (2000) 771.
[35] A.C. Ferrari, A. LiBassi, B.K. Tanner, et al., Phys. Rev. B, submitted.
[36] E.B. Halac, H. Huck, G. Zampieri, R.G. Pergliasco, E. Alonso, M.A.R. de Benycar, Appl. Surf. Sci. 120 (1997) 139.
[37] J. Robertson, C.A. Davis, Diamond Relat. Mater. 4 (1995) 441.
[38] N.V. Sidgwick, The Organic Chemistry of Nitrogen, Oxford Press, Oxford, 1937.